Perturbative calculation of the electromagnetic form factors of the deuteron

David B. Kaplan*
Institute for Nuclear Theory, University of Washington, Seattle, Washington 98195

Martin J. Savage†
Department of Physics, University of Washington, Seattle, Washington 98195

Mark B. Wise‡
California Institute of Technology, Pasadena, California 91125

(Received 8 May 1998)

Making use of the effective field theory expansion recently developed by the authors, we compute the electromagnetic form factors of the deuteron analytically to next-to-leading order. The computation is rather simple, and involves calculating several Feynman diagrams, using dimensional regularization. The results agree well with data and indicate that the expansion is converging. They do not suffer from any ambiguities arising from off-shell versus on-shell amplitudes. [S0556-2813(99)00502-6]

PACS number(s): 13.40.Gp, 13.75.Cs, 12.39.Fe

I. INTRODUCTION

The techniques introduced by the authors in Refs. [1] put the study of low-energy two-nucleon interactions on the same footing as chiral perturbation theory in the mesonic and single nucleon sectors [2]. In particular, there is a systematic low momentum expansion, such that at any given order, one need only calculate a finite number of Feynman diagrams to arrive at an analytic result. The procedure is superior in several ways to the conventional technique of solving the Schrödinger equation with a potential constructed to fit the scattering data: (i) There is a well-defined expansion parameter, and one can estimate errors at any given order in the expansion; (ii) it is straightforward to incorporate relativistic and inelastic effects within the expansion; (iii) analytic results allow one to see quite simply the relative importance of short- and long-distance physics to a given process; (iv) there is no ambiguity concerning off-shell matrix elements when calculating physical processes; (v) at low orders in the expansion, the number of free parameters to be fit to the data is few, and the same parameters are used in all processes. The results at lower orders in the expansion are therefore very constrained.

Until now, the techniques of Ref. [1] have only been applied to reproducing scattering phase shifts. While a necessary first step, fitting the phase shifts does not seriously test the method, as the low-energy phase shifts can be well fit by rather simple functions of few parameters. What is needed are calculations of dynamical processes that involve the same interactions as are fit to the NN phase shifts. The obvious ones to consider are $NN\to NN\gamma$, $np\to d\gamma$, parity and isospin violation in NN processes, $pp\to de^+\nu$, and the deuteron electromagnetic form factors. In this paper we present the perturbative calculation of the deuteron electromagnetic form factors at next-to-leading order (NLO). This subject has been addressed previously in the context of effective field theory in Refs. [3,4], although using a somewhat different formalism and involving numerical, as opposed to analytical, calculations. We preface the calculation with a brief review of our expansion, and a discussion of the deuteron. After identifying the graphs contributing the electromagnetic form factors, we show explicitly that there is no ambiguity arising from the fact that the nucleons in a deuteron are not on their mass shell, even though the couplings in the effective theory are fit to NN scattering data. We conclude with a discussion of features that will appear in the NNLO (next-to-next-to leading order) calculation of the form factors.

It is not unreasonable to ask why it is worth pursuing an effective field theory description of the deuteron since effective range theory [5,6] can be used to predict many of its properties [7,8]. For some quantities, like the deuteron charge radius, effective range theory is remarkably precise. The primary motivation is to make a clear connection to QCD and therefore enable systematic calculations to be performed, even for processes where effective range theory is not applicable. Furthermore we expect that, even in cases where effective range theory is very accurate, the effective field theory approach will surpass this level of precision if pursued to higher orders.

In this paper the application of the effective field theory expansion of Ref. [1] to processes involving the deuteron is developed. For definiteness we focus on the electromagnetic form factors of the deuteron. However, it is straightforward to use the methods developed here for other quantities, like the cross sections for $np\to d\gamma$ and $\gamma d\to\gamma d$.

At NLO the predictions of the effective field theory expansion for the electromagnetic form factors of the deuteron are not as accurate as those of effective range theory. However, at NNLO they should reach the precision of effective range theory. Furthermore, the effective field theory ap-

*Electronic address: dbkaplan@phys.washington.edu
†Electronic address: savage@phys.washington.edu
‡Electronic address: wise@theory.caltech.edu

proach is a systematic one at some order it will include physical effects beyond those that are encorporated into effective range theory.

II. EFFECTIVE FIELD THEORY FOR *NN* INTERACTIONS

In order to compute the electromagnetic form factors of the deuteron, we must consider the possible interactions between nucleons, pions, and photons. In an effective field theory, these interactions take the form of local operators, constrained only by the symmetries of QCD and QED. In this section we discuss the form of the operators that occur to the order that we will be working, and then turn to the issue of power counting, which allows a consistent expansion of the form factors.

A. Interactions

Terms in the effective Lagrangian describing the interactions between nucleons, pions, and photons can be classified by the number of nucleon fields that appear in them. It is convenient to write

$$\mathcal{L}=\mathcal{L}_0+\mathcal{L}_1+\mathcal{L}_2+\cdots, \tag{2.1}$$

where $\mathcal{L}_n$ contains n-body nucleon operators.

$\mathcal{L}_0$ is constructed from the photon field $A^\mu=(A^0,\mathbf{A})$ and the pion fields Π; it does not contain any nucleon fields. The pion fields are incorporated in a special unitary matrix,

$$\Sigma=\exp\frac{2i\Pi}{f},\quad \Pi=\begin{pmatrix}\pi^0/\sqrt{2} & \pi^+\\ \pi^- & -\pi^0/\sqrt{2}\end{pmatrix}, \tag{2.2}$$

where $f=132$ MeV is the pion decay constant. Σ transforms under the global $\mathrm{SU}(2)_L\times\mathrm{SU}(2)_R$ and $\mathrm{U}(1)_{em}$ gauge symmetries as

$$\Sigma\to L\Sigma R^\dagger,\quad \Sigma\to e^{i\alpha Q_{em}}\Sigma e^{-i\alpha Q_{em}}, \tag{2.3}$$

where $L\in\mathrm{SU}(2)_L$, $R\in\mathrm{SU}(2)_R$, and Q_{em} is the charge matrix,

$$Q_{em}=\begin{pmatrix}1 & 0\\ 0 & 0\end{pmatrix}. \tag{2.4}$$

The part of the Lagrange density with no nucleon fields is

$$\mathcal{L}_0=\frac{1}{2}(\mathbf{E}^2-\mathbf{B}^2)+\frac{f^2}{8}\mathrm{Tr}\,D_\mu\Sigma D^\mu\Sigma^\dagger + \frac{f^2}{4}\omega\,\mathrm{Tr}\,m_q(\Sigma+\Sigma^\dagger)+\cdots. \tag{2.5}$$

The ellipsis denotes operators with more covariant derivatives D_μ, insertions of the quark mass matrix, $m_q=\mathrm{diag}(m_u,m_d)$, or factors of the electric and magnetic fields. Acting on Σ the covariant derivative is

$$D_\mu\Sigma=\partial_\mu\Sigma+ie[Q_{em},\Sigma]A_\mu. \tag{2.6}$$

The parameter ω has dimensions of mass and $m_\pi^2=\omega(m_u+m_d)$.

When describing pion-nucleon interactions it is convenient to introduce the field $\xi=\exp i\Pi/f=\sqrt{\Sigma}$. Under $\mathrm{SU}(2)_L\times\mathrm{SU}(2)_R$ transformations

$$\xi\to L\xi U^\dagger=U\xi R^\dagger, \tag{2.7}$$

where U is a complicated nonlinear function of L, R and the pion fields themselves. Since U depends on the pion fields it has spacetime dependence. The nucleon fields are introduced as a doublet of spin-1/2 fields

$$N=\begin{pmatrix}p\\ n\end{pmatrix}, \tag{2.8}$$

that transforms under chiral $\mathrm{SU}(2)_L\times\mathrm{SU}(2)_R$ symmetry as $N\to UN$ and under U(1) gauge transformations as $N\to e^{i\alpha Q_{em}}N$. Acting on nucleon fields the covariant derivative is

$$D_\mu N=(\partial_\mu+V_\mu+ieQ_{em}A_\mu)N, \tag{2.9}$$

where

$$V_\mu=\frac{1}{2}(\xi D_\mu\xi^\dagger+\xi^\dagger D_\mu\xi). \tag{2.10}$$

The covariant derivative of N transforms in the same way as N under $\mathrm{SU}(2)_L\times\mathrm{SU}(2)_R$ transformations (i.e., $D_\mu N\to UD_\mu N$) and under U(1) gauge transformations (i.e., $D_\mu N\to e^{i\alpha Q_{em}}D_\mu N$).

The one-body terms in the Lagrange density are

$$\mathcal{L}_1=N^\dagger\left(iD_0+\frac{\mathbf{D}^2}{2M}\right)N+\frac{ig_A}{2}N^\dagger\boldsymbol{\sigma}\cdot(\xi\mathbf{D}\xi^\dagger-\xi^\dagger\mathbf{D}\xi)N + \frac{e}{2M}N^\dagger\left(\kappa_0+\frac{\kappa_1}{2}[\xi^\dagger\tau^3\xi+\xi\tau^3\xi^\dagger]\right)\boldsymbol{\sigma}\cdot\mathbf{B}N+\cdots. \tag{2.11}$$

To the order to which we are working $\kappa_0=\frac{1}{2}(\kappa_p+\kappa_n)$ and $\kappa_1=\frac{1}{2}(\kappa_p-\kappa_n)$ are isoscalar and isovector nucleon magnetic moments in nuclear magnetons, with

$$\kappa_p=2.792\,85,\quad \kappa_n=-1.913\,04, \tag{2.12}$$

at tree level. At higher orders there will be contributions to Eq. (2.12) from pion loop graphs [9]. The isoscalar magnetic moment κ_0 receives leading corrections of the form $m_\pi^2\ln(m_\pi^2/\Lambda_\chi^2)$, suppressed by two powers of the pion mass. In contrast, the isovector magnetic moment κ_1 receives leading corrections of the form m_π, suppressed by only one power of the pion mass. The ellipsis in Eq. (2.11) denotes higher-order terms that do not contribute at the order we are working.

Finally it remains to consider the two-body operators. Some of these were discussed in Refs. [1]; however, since we will be computing electromagnetic form factors of the deuteron there are additional considerations that did not arise in the NLO calculation of nucleon phase shifts.

First we will consider the two-body operators involving nucleons alone, then we will look at those containing a photon; to the order we will be working, we need not consider two-body operators involving pion fields. In the spin triplet channel, there is one NN contact interaction with no derivatives or insertions of the quark mass matrix, corresponding to a diagonal transition ${}^3S_1 \to {}^3S_1$; the coefficient of this operator is taken to be C_0. There is an additional contact interaction involving no derivatives and one insertion of the quark mass matrix, with coefficient D_2; it can be distinguished from the C_0 interaction by its chiral properties. There are five contact interactions involving two gradients, corresponding to diagonal transitions in the ${}^3S_1$, ${}^3P_0$, ${}^3P_1$, and ${}^3P_2$ partial waves, as well as an off-diagonal ${}^3S_1 - {}^3D_1$ transition. Only the first and the last of these are relevant for the deuteron; furthermore, at NLO we can ignore the ${}^3S_1 - {}^3D_1$ transition interaction. Thus the only ∇^2 two-body contact interaction we will consider is ${}^3S_1 \to {}^3S_1$, and has coupling C_2. Therefore, for a ${}^3S_1 \to {}^3S_1$ scattering process, where the incoming nucleons have momenta $\mathbf{p}_1$, $\mathbf{p}_2$, and polarization i, and scatter into states with momenta $\mathbf{p}_1'$, $\mathbf{p}_2'$, and polarization j, the Born amplitude arising from the contact interactions is

$$i\mathcal{A} = -i\delta_{ij}\left[C_0 + D_2 m_\pi^2 + \frac{C_2}{8}[(\mathbf{p}_1 - \mathbf{p}_2)^2 + (\mathbf{p}_1' - \mathbf{p}_2')^2]\right]. \tag{2.13}$$

The form of the C_2 amplitude is fixed by Lorentz invariance (which is equivalent to Galilean invariance to the order we work), and by the normalization we used in Ref. [1], where in the center-of-mass frame, where we defined the amplitude to be $-iC_2 p^2$, $p \equiv |\mathbf{p}_i| = |\mathbf{p}_i'|$.[1] As discussed in Appendix B, while one can construct a two-body contact interaction with one factor of ∂_0 instead of two gradients, for any S-matrix element (including those involving the deuteron) one can use the equations of motion to eliminate time derivatives for gradients. Thus no independent ∂_0 contact interaction needs to be introduced.

Including gauge fields introduces several two-body contributions to the electromagnetic current. First, the C_2 interaction described above becomes gauged. Second, there are two new two-body magnetic moment type interactions. In order to write $\mathcal{L}_2$ compactly we define the matrix P_i which projects onto the ${}^3S_1$ state,

$$P_i \equiv \frac{1}{\sqrt{8}}\sigma_2\sigma_i\tau_2, \quad \mathrm{Tr}\, P_i^\dagger P_j = -\mathrm{Tr}\, P_i^\dagger P_j^T = \frac{1}{2}\delta_{ij}, \tag{2.14}$$

where the σ matrices act on the nucleon spin indices, while the τ matrices act on isospin indices. Then the two-body Lagrangian may be written as

$$\begin{aligned}\mathcal{L}_2 = &-(C_0 + D_2\omega\,\mathrm{Tr}\, m_q)(N^T P_i N)^\dagger (N^T P_i N) \\ &+ \frac{C_2}{8}[(N^T P_i N)^\dagger (N^T[P_i \vec{\mathbf{D}}^2 + \overleftarrow{\mathbf{D}}^2 P_i - 2\overleftarrow{\mathbf{D}} P_i \vec{\mathbf{D}}]N) + \mathrm{H.c.}] \\ &+ eL_2[(N^T P_i N)^\dagger (N^T P_i \boldsymbol{\sigma}\cdot\mathbf{B} N) + \mathrm{H.c.}] + \cdots,\end{aligned} \tag{2.15}$$

where the ellipsis refers to contact interactions irrelevant for the deuteron channel, or of higher order than we will be considering. The new coupling L_2 corresponds to an interaction that did not enter the calculation of NN scattering, but which affects the deuteron magnetic form factor. As written, Eq. (2.15) is not chirally invariant, which can be remedied by an appropriate insertion of the ξ fields; however, since the two-body operators with pions do not contribute at NLO, we omit them.

B. Power counting

We begin by summarizing the results of Refs. [1]. The starting point is the effective Lagrangian for nucleons, pions, and photons introduced in the previous section. The part of the Lagrangian describing purely mesonic interactions, as well as interactions between mesons and a single baryon, is the conventional chiral Lagrangian. In addition there are local interactions corresponding to short distance interactions between two nucleons. These contact interactions are expanded in powers of derivatives and insertions of the quark mass matrix, m_q. (Isospin violation from the difference between the up and down quark masses is neglected. Consequently insertions of m_q are equivalent to factors of m_π^2.) The lowest dimension operator is a four fermion contact interaction; there are two independent operators of this form, corresponding to the ${}^1S_0$ and ${}^3S_1$ channels. The next lowest dimension two-body operators involve a factor of p^2, where p is the momentum of one of the nucleons in the center-of-mass frame, or a factor of m_π^2. There are seven independent p^2 operators corresponding to diagonal matrix elements in the $\{{}^1S_0, {}^1P_1, {}^3S_1, {}^3P_0, {}^3P_1, {}^3P_2\}$ channels, as well as a ${}^3S_1 - {}^3D_1$ mixing term; there are two independent m_π^2 operators corresponding to the ${}^1S_0$ and ${}^3S_1$ channels. At higher powers of derivatives, the number of contact interactions quickly grows.

Central to effective field theory is a power counting scheme which allows one to calculate consistently to any given order in the low energy expansion. A main point in Refs. [1] was to develop the PDS subtraction scheme which allows one to readily identify the order of any particular Feynman graph. The scheme involves computing loop diagrams using dimensional regularization, and then subtracting off the poles in dimensions $D \leqslant 4$, which correspond to logarithmic or power-law divergences. A typical integral in this scheme is

[1]The couplings C_0, D_2, and C_2 are the same couplings that appear as $C_0^{({}^3S_1)}$, $D_2^{({}^3S_1)}$, and $C_2^{({}^3S_1)}$ in Refs. [1]; we drop the ${}^3S_1$ designation here as there can be no confusion with analogous couplings in the ${}^1S_0$ channel.

$$I_n \equiv i(\mu/2)^{4-D}\int \frac{d^Dq}{(2\pi)^D}\mathbf{q}^{2n}(E/2+q_0-\mathbf{q}^2/2M+i\varepsilon)^{-1}(E/2-q_0-\mathbf{q}^2/2M+i\varepsilon)^{-1}$$

$$=(\mu/2)^{4-D}\int \frac{d^{(D-1)}\mathbf{q}}{(2\pi)^{(D-1)}}\mathbf{q}^{2n}(E-\mathbf{q}^2/M+i\varepsilon)^{-1}$$

$$=-M(ME)^n(-ME-i\varepsilon)^{(D-3)/2}\Gamma\left(\frac{3-D}{2}\right)\frac{(\mu/2)^{4-D}}{(4\pi)^{(D-1)/2}}$$

$$\underset{D\to 4}{\overset{PDS}{\to}} -(ME)^n\left(\frac{M}{4\pi}\right)(\mu-\sqrt{-ME-i\varepsilon}). \tag{2.16}$$

The last step includes the finite subtraction mandated in the *PDS* scheme. The parameter μ is the renormalization scale and physical observables are independent of it. In fact, one may set μ to zero and recover the usual minimal subtraction scheme (MS) with $\mu=0$ if one wishes.[2] However, a change in μ must be compensated by the renormalization-group flow of the couplings in the theory. Therefore, what is a weak coupling at one value of μ can be strong at another, which effects how one defines the power counting scheme.

Rapid scaling with μ is only an issue for two-body operators, and then only for those affected by the large scattering lengths in the ${}^1S_0$ and ${}^3S_1$ channels. Consider a four nucleon contact interaction connecting angular momentum states L and L', where conservation of angular momentum and parity requires $|L-L'|$ to equal zero or two. We assume that the operator involves m insertions of the quark mass matrix, and $2d\equiv(L+L'+2n)$ spatial gradients, and has a coefficient $C_{m,n}^{L,L'}$. By examining the coupled renormalization-group equations in the *PDS* scheme, one can determine that these couplings scale as

$$C_{m,n}^{L,L'}(\mu)\sim\begin{cases}\mu^{-(m+n+1)} & L,L'\in\{{}^1S_0,{}^3S_1,{}^3D_1\};\\ \mu^0, & \text{otherwise,}\end{cases} \tag{2.17}$$

in the region $1/a\ll\mu\ll\Lambda_{NN}$, where

$$\Lambda_{NN}=\frac{8\pi f^2}{g_A^2 M}\simeq 300 \quad \text{MeV}. \tag{2.18}$$

Here M is the nucleon mass, $g_A=1.25$ is the axial current coupling, and $f=132$ MeV is the pion decay constant. Thus in the deuteron channel, $C_0\sim\mu^{-1}$, while C_2 and D_2 scale as μ^{-2}. Extending the analysis to include photons, we find $L_2\sim\mu^{-2}$ as well.

The coefficients of the four-nucleon contact terms that have explicit factors of the electric field **E** or the magnetic field **B** scale similarly to those in Eq. (2.17), counting gauge fields as derivatives. For example, the L_2 operator in Eq. (2.15) counts as a two-derivative, $L=L'=0$ operator, and its coefficient scales as $L_2\sim\mu^{-2}$. The rapid scaling of the operators contributing to *S*-wave processes is what makes our expansion different than the one proposed by Weinberg [10].

Armed with the above results, we are able to arrive at a particularly simple set of rules for determining the order of a graph. Choosing the scale $\mu\sim p\sim m_\pi\sim Q$ we perform an expansion in Q, where

(1) Each nucleon or pion propagator scales as Q^{-2};

(2) Each loop integration $\int d^4q$ scales as Q^5;

(3) A gradient at a vertex contributes Q^1, while each time derivative scales as Q^2;

(4) An insertion of the quark mass matrix m_q at a vertex counts as Q^2;

(5) The coefficient of the contact interactions scale according to Eq. (2.17).

The first three rules follow simply from the scaling of four momenta q_μ appropriate to the nonrelativistic regime. Explicitly, $Mq_0\sim\mathbf{q}^2\sim Q^2$. The fourth rule is familiar from conventional chiral perturbation theory, $m_q\sim m_\pi^2\sim Q^2$. The procedure for calculating physical quantities of interest is to write down the most general effective field theory consistent with gauge invariance, chiral symmetry, and Lorentz invariance,[3] and then compute the desired matrix element to a given order in the Q expansion, following the above rules. Note that according to the power counting rules, a loop with two propagators entails a factor of Q, while the coefficient of the lowest order NN contact interaction ($C_{d,m}^{LL'}$ with $L=L'=d=m=0$, defined to be C_0) scales as $1/Q$; thus any graph may be dressed by an infinite bubble chain with C_0 interactions without changing the order of the graph.

III. THE DEUTERON FORM FACTORS

A deuteron with four momentum p^μ and polarization vector ϵ^μ is described by the state $|\mathbf{p},\epsilon\rangle$, where the polarization vector satisfies $p_\mu\epsilon^\mu=0$. An orthonormal basis of polarization vectors ϵ_i^μ satisfies

[2]In the MS scheme with $\mu=0$ one must first integrate out the pion to avoid factors that diverge as $\ln(m_\pi^2/\mu^2)$.

[3]Relativistic corrections are accounted for as perturbations according to the above power counting rules, and at the order we work the theory only appears Galilean invariant. The procedure for dealing with relativistic corrections perturbatively requires distinguishing between potential and radiation pions at NNLO, as discussed in [1].

$$p_\mu \epsilon_i^\mu = 0, \quad \epsilon_{i\mu}^* \epsilon_j^\mu = -\delta_{ij}, \quad \sum_{i=1}^{3} \epsilon_i^{*\mu} \epsilon_i^\nu = \frac{p^\mu p^\nu}{M_d^2} - \eta^{\mu\nu}, \tag{3.1}$$

where M_d is the deuteron mass. It is convenient to choose the basis polarization vectors so that in the deuteron rest frame $\epsilon_i^\mu = \delta_i^\mu$. Deuteron states with these polarizations are denoted by $|\mathbf{p},i\rangle$ (i.e., $|\mathbf{p},i\rangle \equiv |\mathbf{p},\epsilon_i^\mu\rangle$) and satisfy the normalization condition

$$\langle \mathbf{p}',j|\mathbf{p},i\rangle = \frac{p^0}{M_d}(2\pi)^3 \delta^3(\mathbf{p}-\mathbf{p}')\,\delta_{ij}. \tag{3.2}$$

In terms of these states and to leading order in the nonrelativistic expansion, the matrix element of the electromagnetic current is

$$\langle \mathbf{p}',j|J_{em}^0|\mathbf{p},i\rangle = e\left[F_C(q^2)\,\delta_{ij} + \frac{1}{2M_d^2}F_{\mathcal{Q}}(q^2) \times \left(\mathbf{q}_i\mathbf{q}_j - \frac{1}{3}\mathbf{q}^2\delta_{ij}\right)\right],$$

$$\langle \mathbf{p}',j|\mathbf{J}_{em}^k|\mathbf{p},i\rangle = \frac{e}{2M_d}\Bigg[F_C(q^2)\,\delta_{ij}(\mathbf{p}+\mathbf{p}')^k + F_M(q^2) \times (\delta_j^k\mathbf{q}_i - \delta_i^k\mathbf{q}_j) + \frac{1}{2M_d^2}F_{\mathcal{Q}}(q^2) \times \left(\mathbf{q}_i\mathbf{q}_j - \frac{1}{3}\mathbf{q}^2\delta_{ij}\right)(\mathbf{p}+\mathbf{p}')^k\Bigg], \tag{3.3}$$

where $\mathbf{q}=\mathbf{p}'-\mathbf{p}$ and $q=|\mathbf{q}|$. These dimensionless form factors are normalized such that [11]

$$F_C(0)=1,$$

$$\frac{e}{2M_d}F_M(0)=\mu_M, \tag{3.4}$$

$$\frac{1}{M_d^2}F_{\mathcal{Q}}(0)=\mu_{\mathcal{Q}},$$

where $\mu_M = 0.857\,41(e/2M)$ is the deuteron magnetic moment, and $\mu_{\mathcal{Q}} = 0.2859$ fm^2 is the deuteron quadrupole moment.

As shown in Appendix A, the form factors are readily calculated by computing in perturbation theory the irreducible two-point function Σ, and the irreducible three-point function Γ^μ. In the present context, ''irreducible'' means the sum of graphs which do not fall apart when cut at any C_0 vertex. The matrix element of the electromagnetic current is then given by the exact relation

$$\langle \mathbf{p}',j|J_{em}^\mu|\mathbf{p},i\rangle = i\left[\frac{\Gamma_{ij}^\mu(\bar{E},\bar{E}',\mathbf{q})}{d\Sigma(\bar{E})/dE}\right]_{\bar{E},\bar{E}'\to -B}, \tag{3.5}$$

where B is the deuteron binding energy and $\bar{E}$ is the energy of the incoming two nucleon state in the center-of-mass frame,

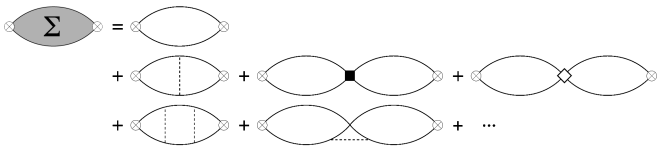

FIG. 1. The perturbative expansion of Σ. The first row has the leading $O(Q)$ result; $\otimes$ represents an insertion of the interpolating field defined in Eq. (3.7). The second row has the complete subleading $O(Q^2)$ contribution, where $\blacksquare$ and $\diamond$ denote the C_2 and D_2 interactions, respectively. The third row shows a couple of $O(Q^3)$ NNLO contributions, which we do not calculate here: the exchange of two potential pions, and the dressing of C_0 (the pointlike NN vertex) by a radiation pion.

$$\bar{E} \equiv E - \frac{\mathbf{p}^2}{4M} + \cdots, \quad E \equiv (p^0 - 2M), \tag{3.6}$$

where the ellipsis refers to relativistic corrections to the energy-momentum relation. $\bar{E}'$ is the analogous quantity for the outgoing nucleon pair. By Lorentz invariance, Σ and Γ^μ can only depend on the energy and momentum in this combination.

We can now expand the relation Eq. (3.5) in perturbation theory and determine the form factors by comparing the result with Eq. (3.3). The two-point function has the graphical expansion shown in Fig. 1, where the $\otimes$ vertices represent the insertion of an interpolating field $\mathcal{D}_i$ with the quantum numbers of a deuteron with polarization i. We take $\mathcal{D}_i$ to be

$$\mathcal{D}_i \equiv N^T P_i N, \tag{3.7}$$

where P_i is the projection defined in Eq. (2.14). The form factor one calculates does not depend on the particular choice for $\mathcal{D}_i$, so long as it is used consistently.

By examining the graphs and using the power counting outlined in the previous section, one sees that Σ begins at order Q^1—the leading graph has two nucleon propagators and one loop. At subleading order, $O(Q^2)$, there are three two-loop graphs, one involving the exchange of a potential pion (which has a derivative coupling), one with an insertion of the $C_2(\overleftrightarrow{\mathbf{D}})^2$ two-body operator, and one with an insertion of the $D_2 m_\pi^2$ two-body operator. Recall that with renormalization scale $\mu \sim Q$ the coefficients C_2 and D_2 are $O(Q^{-2})$. At $O(Q^3)$ there are a host of diagrams, including the exchange of two potential pions, or one radiative pion, as well as $\mathbf{p}^4$ relativistic corrections to the nucleon propagator, etc. We have calculated Σ to $O(Q^2)$, and the results are presented in Appendix A.

A. The NLO computation of the electric form factors

To compute the electric form factors F_C and $F_{\mathcal{Q}}$ we need to calculate the three-point function Γ_{ij}^0, which is expanded graphically in Fig. 2. The results for both the leading $O(Q^{-1})$ and subleading $O(Q^0)$ contributions are presented in Appendix A. Once Γ^0 is computed in the Q expansion, the electric form factors can be determined by expanding Eq. (3.5) as

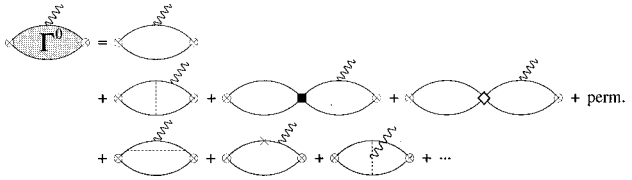

FIG. 2. The expansion of Γ^0. In all of these graphs, the photon corresponds to A_0 with the minimal coupling to the proton propagator, arising from the gauged nucleon kinetic energy term. The graph in the first row is the leading $O(Q^{-1})$ contribution, $\Gamma^0_{(-1)}$. The second row is the subleading graphs at $O(Q^0)$, summing to give $\Gamma^0_{(0)}$. In the third row are several graphs contributing at the $O(Q^1)$: a dressing of the photon-nucleon vertex, a relativistic correction to the nucleon propagator, and an exchange current contribution.

$$\langle \mathbf{p}',j|J^0_{em}|\mathbf{p},i\rangle = i\left[\frac{\Gamma^0_{(-1)}}{d\Sigma_{(1)}/d\bar{E}}\right] + i\left[\frac{\Gamma^0_{(0)}(d\Sigma_{(1)}/d\bar{E})-\Gamma^0_{(-1)}(d\Sigma_{(2)}/d\bar{E})}{(d\Sigma_{(1)}/d\bar{E})^2}\right] + O(Q^2), \tag{3.8}$$

where $\Gamma^0_{(n)}$, $\Sigma_{(n)}$ denote the $O(Q^n)$ contribution to Γ^0 and Σ, respectively. We have suppressed the $\mathbf{q}$ dependence of Γ^0, and its polarization indices. Furthermore everything is evaluated on-shell, $\bar{E}=\bar{E}'=-B$. Since $d/d\bar{E}\sim O(Q^{-2})$, the first bracket in Eq. (3.8) is $O(Q^0)$, the second bracket is $O(Q^1)$, etc. Therefore, taking into account the explicit factors of q in the definition of the form factors, Eq. (3.3), we see the electric form factors have a Q expansion of the form

$$F_C = F_C^{(0)} + F_C^{(1)} + O(Q^2),$$
$$F_{\mathcal{Q}} = F_{\mathcal{Q}}^{(-2)} + F_{\mathcal{Q}}^{(-1)} + O(Q^0), \tag{3.9}$$

where $F^{(n)}\sim O(Q^n)$.

Using Eqs. (3.8),(A6),(A17) gives our leading result for the electric form factors,

$$F_C^{(0)}(q^2) = \frac{4\gamma}{q}\tan^{-1}\left(\frac{q}{4\gamma}\right),$$
$$F_{\mathcal{Q}}^{(-2)}(q^2) = 0, \tag{3.10}$$

where we have defined

$$\gamma = \sqrt{MB}. \tag{3.11}$$

The subleading form factors are extracted from Eqs. (3.8),(A6),(A18), and presented in terms of a Feynman parameter integral. The electric monopole form factor is given by

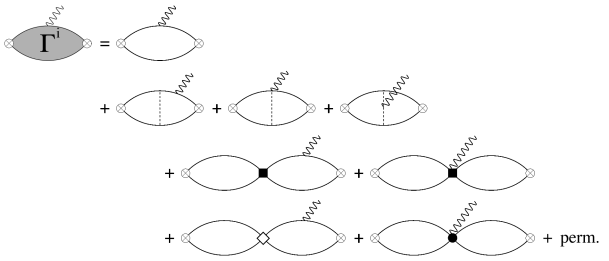

FIG. 3. The expansion of Γ^i, where the photon corresponds to the vector potential $\mathbf{A}^i$. The coupling of the photon to the nucleon lines represents the entire one-body current from $\mathcal{L}_1$, Eq. (2.11), including the magnetic moment contribution. The first graph is the LO contribution at $O(Q^0)$, while the remaining graphs are the NLO contributions at $O(Q^1)$. The photon couplings arise through any of the operators in $\mathcal{L}_0$, $\mathcal{L}_1$, or $\mathcal{L}_2$. We specifically distinguish the C_2, D_2, and L_2 vertices by the symbols ■, ◇, and ●, respectively.

$$F_C^{(1)}(q^2) = -C_2(\mu)\frac{M\gamma(\mu-\gamma)^2}{2\pi}\left[1-\frac{4\gamma}{q}\tan^{-1}\left(\frac{q}{4\gamma}\right)\right] - \frac{g_A^2 M m_\pi^2\gamma}{2\pi f^2 q}\left[\frac{2}{(m_\pi+2\gamma)}\tan^{-1}\left(\frac{q}{4\gamma}\right) - \int_0^1 dx\,\frac{1}{x\Delta}\tan^{-1}\beta\right], \tag{3.12}$$

where we have defined the functions

$$\Delta(x) = \sqrt{\gamma^2 + x(1-x)q^2/4}, \quad \beta(x) = \frac{qx}{2(\gamma+m_\pi+\Delta)}. \tag{3.13}$$

The operator with coefficient D_2 does not contribute to these observables. Because of the running of C_2, the above expression is independent of μ to the order we are working [1]. From Eqs. (3.10)–(3.12) we determine the charge radius of the deuteron to NLO,

$$\langle r^2\rangle^{\rm LO} = \frac{1}{8\gamma^2},$$
$$\langle r^2\rangle^{\rm NLO} = C_2(\mu)\frac{M(\mu-\gamma)^2}{16\pi\gamma} + \frac{g_A^2 M m_\pi^2(3m_\pi+10\gamma)}{96\pi f^2\gamma(m_\pi+2\gamma)^3}. \tag{3.14}$$

A comparison with the experimental value is given in Sec. IV.

At NLO, the electric quadrupole form factor is given by

$$\frac{F_{\mathcal{Q}}^{(-1)}(q^2)}{M_d^2}=\frac{3g_A^2M\gamma}{16\pi f^2q^3}\int_0^1 dx\frac{1}{x\beta^4\Delta}([3q^2x^2(1+\beta^2)^2-24qm_\pi\beta x(1+\beta^2)+16m_\pi^2\beta^2(3+\beta^2)]\tan^{-1}\beta$$
$$+\beta[-48m_\pi^2\beta^2+8m_\pi qx\beta(3+2\beta^2)-q^2x^2(3+5\beta^2)]). \tag{3.15}$$

From this expression one can extract the quadrupole moment to first nonvanishing order:

$$\mu_{\mathcal{Q}}^{\rm LO}=0,\quad \mu_{\mathcal{Q}}^{\rm NLO}=\frac{g_A^2M(6\gamma^2+9\gamma m_\pi+4m_\pi^2)}{30\pi f^2(m_\pi+2\gamma)^3}. \tag{3.16}$$

A comparison with the experimental value is given in Sec. IV.

B. The NLO computation of the magnetic form factor

In order to calculate the magnetic form factor of the deuteron, we need the matrix element of the spatial current $\langle \mathbf{p}',k|\mathbf{J}_{em}^i|\mathbf{p},j\rangle$. This entails computing Γ^i, using the coupling of the spatial component of the gauge field $\mathbf{A}_i$, discussed in Sec. II A. The expansion of Γ^i in Feynman graphs is shown to subleading order in Fig. 3. Following our power counting rules, Γ^i begins at $O(Q^0)$, and so an expansion analogous to Eq. (3.8) for the matrix element of $\mathbf{J}_{em}^i$ implies that the magnetic form factor has the expansion

$$F_M=F_M^{(0)}+F_M^{(1)}+O(Q^2). \tag{3.17}$$

Our task in computing F_M is greatly simplified by recognizing from Eq. (3.3) that we need only pick out contributions with spin structure antisymmetric in the deuteron polarization vectors. It is straightforward to check that none of the graphs shown in Fig. 3 contribute to F_M when the photon coupling arises from any of the operators $N^\dagger\mathbf{D}^2N$, $g_AN^\dagger\boldsymbol{\sigma}\cdot(\xi\mathbf{D}\xi^\dagger-\xi^\dagger\mathbf{D}\xi)N$, $\mathrm{Tr}[D_\mu\Sigma D^\mu\Sigma^\dagger]$ in Eq. (2.11), or the four-nucleon operator with coefficient C_2 in Eq. (2.15). At LO, only the photon coupling via the isosinglet nucleon magnetic moment one-body operator contributes,

$$\frac{e}{2M}\kappa_0N^\dagger\boldsymbol{\sigma}\cdot\mathbf{B}N=\frac{\mu_p+\mu_n}{2}N^\dagger\boldsymbol{\sigma}\cdot\mathbf{B}N, \tag{3.18}$$

and we find

$$\frac{eF_M^{(0)}(q^2)}{2M_d}=\frac{e}{M}\kappa_0F_C^{(0)}(q^2)=(\mu_p+\mu_n)\frac{4\gamma}{q}\tan^{-1}\left(\frac{q}{4\gamma}\right). \tag{3.19}$$

For the deuteron magnetic moment this gives $\mu_M^{\rm LO}=(\mu_p+\mu_n)$, simply the sum of the neutron and proton magnetic moments.

At next order Q^1 there are contributions to F_M arising from coupling the photon via Eq. (3.18), along with insertions of the C_2 operator or one-pion exchange; there is also a contribution from the two-body current arising from the operator in Eq. (2.15) whose coefficient is L_2. We find that there are no pion exchange current contributions at this order, nor any two-body current contribution from the C_2 operator in Eq. (2.15). With the exception of the two-body contribution involving an explicit factor of $\mathbf{B}$ [see Eq. (2.15)], all the graphs contributing are all proportional to those giving rise to the electric form factors in Fig. 2. Therefore to this order we can express the magnetic form factor in terms of the electric form factors and a single new coupling constant. We find

$$\frac{eF_M^{(1)}(q^2)}{2M_d}=(\mu_p+\mu_n)\left(F_C^{(1)}(q^2)+\frac{q^2}{12M_d^2}F_{\mathcal{Q}}^{(-1)}(q^2)\right)$$
$$+eL_2\frac{\gamma}{\pi}(\mu-\gamma)^2, \tag{3.20}$$

and the deuteron magnetic moment is given by

$$\mu_M^{\rm LO}=\mu_p+\mu_n,$$
$$\mu_M^{\rm NLO}=eL_2\frac{\gamma}{\pi}(\mu-\gamma)^2, \tag{3.21}$$

where L_2 depends on the renormalization scale μ in such a way that $\mu_M^{(1)}$ is μ independent. A comparison with the experimental value is given in the next section.

C. Effective range theory

In effective range theory the electromagnetic form factors are assumed to be dominated by the asymptotic S-wave deuteron wave function,

$$\psi^{(\rm ER)}(\mathbf{r})=\sqrt{\frac{\gamma}{4\pi(1-\gamma r_0)}}\frac{e^{-\gamma r}}{r}. \tag{3.22}$$

Assuming the small r part of the deuteron wave function is only important for establishing the normalization condition, $F_C(0)=1$, the prediction of effective range theory for the form factor $F_C(q^2)$ follows from the Fourier transform of $|\psi^{(\rm ER)}(\mathbf{r})|^2$,

$$F_C^{(\rm ER)}(q^2)=1+\left(\frac{1}{1-\gamma r_0}\right)\left[-1+\frac{4\gamma}{q}\tan^{-1}\left(\frac{q}{4\gamma}\right)\right]. \tag{3.23}$$

This yields the charge radius

$$\langle r^2\rangle^{\rm ER}=\frac{1}{8\gamma^2}\frac{1}{1-\gamma r_0}=\frac{1}{8\gamma^2}[1+\gamma r_0+\gamma^2r_0^2+\cdots]. \tag{3.24}$$

It is instructive to compare the effective range theory prediction for the charge radius with that from effective field theory. In effective field theory at NLO the effective range is ($r_0=0$ at LO),

TABLE I. Electromagnetic properties of the deuteron.

	LO	NLO	(LO+NLO)	Experiment [12,13]
rms charge radius (fm)	1.53	0.36	1.89	2.1303(66)
Magnetic moment (N.M.)	0.88	−0.02 (fit)	0.86 (fit)	0.85741
Quadrupole moment (fm^2)		0.40	0.40	0.2859(3)

$$r_0 = C_2(\mu)\frac{M(\mu-\gamma)^2}{2\pi} + \frac{g_A^2 M}{4\pi f^2}\left(1 - \frac{8}{3}\frac{\gamma}{m_\pi} + 2\frac{\gamma^2}{m_\pi^2}\right). \tag{3.25}$$

Using this it is straightforward to show that the γ expansion of the NLO effective field theory charge radius,

$$\begin{aligned}\langle r^2\rangle &= \frac{1}{8\gamma^2}\left[1 + C_2(\mu)\frac{M\gamma(\mu-\gamma)^2}{2\pi} + \frac{g_A^2 M\gamma m_\pi^2(3m_\pi+10\gamma)}{12\pi f^2(m_\pi+2\gamma)^3}\right] \\ &= \frac{1}{8\gamma^2}\left[1 + C_2(\mu)\frac{M\gamma(\mu-\gamma)^2}{2\pi} + \frac{g_A^2 M\gamma}{4\pi f^2}\left(1 - \frac{8}{3}\frac{\gamma}{m_\pi} + 4\frac{\gamma^2}{m_\pi^2} + \cdots\right)\right],\end{aligned} \tag{3.26}$$

and the γ expansion of effective range theory agree to order γ^2 at linear order in r_0.

Effective range theory predicts the matter radius r_m with remarkable precision. Using $r_0 = 1.75$ fm effective range theory yields $r_\mathrm{m}^{(\mathrm{ER})} = 1.98$ fm. The most recent measurement of the deuteron charge radius is $r_\mathrm{ch} = 2.1303 \pm 0.0066$ fm from which the matter radius is found to be $r_\mathrm{m} = 1.9685 \pm 0.0049$ fm [12]. (In effective field theory the effects that distinguish between the matter and charge radius do not arise until NNLO.) The numerical success of the prediction of effective range theory for the matter radius suggests that the most important higher-order terms in effective field theory are those that arise from iterating the NLO potential from C_2 and one-pion exchange. However, from the effective field theory perspective this cannot be justified since there are new local operators that will contribute at the same order.

Effective range theory can also be used to predict the magnetic form factor and it gives

$$\frac{eF_M^{(\mathrm{ER})}(q^2)}{2M_d} = (\mu_p + \mu_n)F_C^{(\mathrm{ER})}(q^2). \tag{3.27}$$

In the following section $F_C^{(\mathrm{ER})}(q^2)$ and $F_M^{(\mathrm{ER})}(q^2)$ are compared with experimental data.

IV. COMPARISON WITH DATA

We now compare the analytic results of our effective field theory perturbative expansion for the deuteron form factors with experimental data. We have evaluated these expressions at the same renormalization point $\mu = m_\pi$ used in Refs. [1] and have used the same value

$$C_2(m_\pi) = 9.91 \ \mathrm{fm}^4 \tag{4.1}$$

derived from a fit to the NN scattering phase shifts in the spin-triplet channel. The values of C_0 and D_2 do not enter our expressions explicitly, but they do enter indirectly through the constraint on the two-point function that the deuteron pole occurs at the correct binding energy, Eq. (A6). Given C_2 from the NN phase-shift analysis, we have no new parameters at NLO for fitting the electric form factors. As we have seen, for the magnetic form factor, a single new parameter L_2 enters at NLO.

We first consider that static moments of the deuteron, at $q^2 = 0$. We have analytic formulas for the charge radius, the quadrupole moment, and the magnetic moment in Eqs. (3.14), (3.16), and (3.21), respectively. A comparison of these values to experiment is given in Table I. The charge radius shows a rapid convergence to the measured value, which is encouraging. The LO calculation is expected to be within ~30% of the experimental value, while the NLO calculation is expected to be within ~10%. It is clear from Table I that this expectation is fulfilled. When the NNLO calculation is performed we expect that the result is within ~3% of the experimental value. The magnetic moment agrees well with experiment at LO, and then is fit to the experimental value at NLO by choosing the strength L_2 of the two-body magnetic operator appropriately. The LO prediction for the magnetic moment is much closer to the experimental value (within ~3%) than naively expected from the power counting. The quadrupole moment vanishes at LO, and the NLO value of 0.40 fm^2 is off by ~40%, as expected from the power counting. It would be useful to compute the NNLO contribution to μ_Q to see if it exhibits the same convergence as the charge radius. The idea of including pions perturbatively has been used previously to estimate the deuteron quadrupole moment [14], obtaining a value of 0.40 fm^2. More interesting is that iterated potential pion exchange reproduces the deuteron quadrupole moment [8] reasonably well. This suggests that contributions to the quadrupole moment from higher-order counterterms are small compared to additional insertions of potential pion exchange. This smallness is not something that arises naturally in the effective field theory. It is also interesting that state-of-the-art nuclear calculations of the quadrupole moment [15] (~0.270 fm^2) are systematically lower than the experimental value by ~7%. This strongly suggests that dynamics beyond potential interactions are required, something that effective field theory provides a systematic way to include.

Of greater interest is the comparison of the form factors over a range of q^2, as we should be able to see at what momentum the expansion begins to fail; our naive estimate is that the expansion is in powers of $q/2\Lambda_{NN} \sim q/(600\ \mathrm{MeV})$. The differential cross section for elastic electron-deuteron scattering is given by

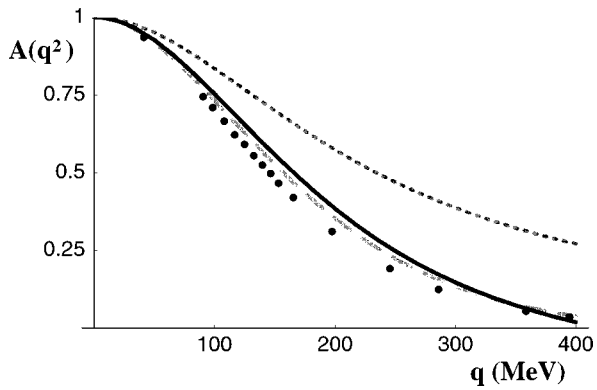

FIG. 4. A plot of $A(q^2)$ vs q in MeV for elastic electron-deuteron scattering. The dotted curve shows the result of the LO calculation, while the solid curve is the NLO prediction. There are no free parameters at this order. The dashed curve shows the result of effective range theory.

$$\frac{d\sigma}{d\Omega}=\left.\frac{d\sigma}{d\Omega}\right|_{\text{Mott}}[A(q^2)+B(q^2)\tan^2\theta/2], \tag{4.2}$$

where A and B are related to the form factors [11]:

$$A=F_C^2+\frac{2}{3}\eta F_M^2+\frac{8}{9}\eta^2 F_Q^2,$$

$$B=\frac{4}{3}\eta(1+\eta)F_M^2, \tag{4.3}$$

with $\eta\equiv-(p-p')^2/(4M_d^2)\simeq q^2/4M_d^2$. In order to compare with data, we take our analytic results for the form factors and expand the expression Eq. (4.3) in powers of Q, where $\eta\sim O(Q^2)$

$$A=[(F_C^{(0)})^2]+[2F_C^{(0)}F_C^{(1)}]+O(Q^2),$$

$$B=\left[\frac{4}{3}\eta(F_M^{(0)})^2\right]+\left[\frac{8}{3}\eta F_M^{(0)}F_M^{(1)}\right]+O(Q^4). \tag{4.4}$$

We see that to the order we are working, A is sensitive only to the electric form factor F_C, while B depends only on the magnetic form factor F_M. A comparison of A and B with experimental data in Figs. 4 and 5 shows that our expansion is quite successful, and converging rapidly, in the kinematic regime where it is expected to work. The data for Fig. 4 was taken from Ref. [16], and the error bars are smaller than the size of the points; the data for Fig. 5 comes from Refs. [16–19]. It is evident from Figs. 4 and 5 that the NLO effective field theory calculation of the deuteron form factors is not as accurate as what effective range theory gives. The validity of effective range theory over such a wide range of momentum occurs because of the smallness of the shape parameter r_1. In the effective field theory expansion, the coefficients in the effective range expansion themselves have perturbative expansions. However, ultimately when carried out to higher orders the effective field theory calculations will be more precise than the effective range calculations. This is because the effective field theory correctly describes the strong interactions, which effective range theory only approximates.

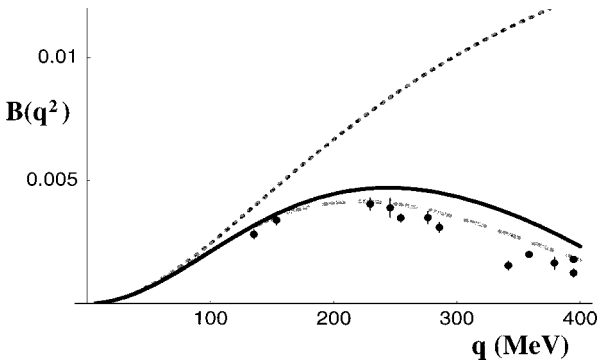

FIG. 5. A plot of $B(q^2)$ vs q in MeV for elastic electron-deuteron scattering. The dotted curve shows the result of the LO calculation, while the solid curve is the NLO prediction. There is one free parameter at this order L_2, which is fixed to correctly reproduce the deuteron magnetic moment. The dashed curve shows the result of effective range theory.

V. CONCLUSIONS

We have demonstrated that one can compute properties of the two-nucleon system to surprising accuracy simply by calculating several Feynman diagrams. The technique for doing this was introduced in Refs. [1] where it had been shown how to work at NLO for NN phase shifts in both spin singlet and triplet channels. While encouraging, those results were not definitive as the NLO calculation required three free parameters in both spin channels. The true test of the theory has been presented in this paper with the computation of the electromagnetic form factors of the deuteron — by using the parameters fit to scattering data, we are able to reproduce very well at NLO both the electric and magnetic form factors in elastic $e-d$ scattering up to momentum transfers $q^2=(400\ \text{MeV})^2=4.1\ \text{fm}^{-2}$. Since our results are analytic, it is straightforward to analyze what features in the data are due to short versus long distance physics. A central feature of our expansion — that pion exchange is perturbative — is supported by the success of our fit to the form factors.

One feature of our results which is especially encouraging is the evidence that the expansion is converging rapidly. This is apparent in the improvement of the fits to $e-d$ scattering data in going from LO to NLO, improvements in the static moments of the deuteron. The rms charge radius presented in Table I deviates from the experimental value by $\sim 30\%$ at leading order, but only $\sim 10\%$ at next-to-leading order. The magnetic moment was off by $\sim 3\%$ at leading order, and exact at next-to-leading order, due to the contribution of a new operator. At NLO the results of effective field theory for the electric and magnetic form factors of the deuteron, $F_C(q^2)$ and $F_M(q^2)$, are not as accurate as those from effective range theory. However at NNLO the effective field theory approach should reach (or even surpass) the precision of effective range theory. Furthermore, the methods developed in this paper can be used to make predictions for other properties of the deuteron, including those for which effective range theory is not applicable.

Since the NLO result for the quadrupole form factor is the first nonvanishing term in its expansion, it is expected to work less well. At the level we are working, the quadrupole form factor does not contribute to $e-d$ scattering, however, we can compare the quadrupole moment with experiment,

and it is $\sim 40\%$ too large. We expect this error to be substantially reduced in the NNLO calculation, which includes among other things the exchange of two potential pions, and short distance ${}^3S_1 - {}^3D_1$ transitions. In general, it would be interesting to compare NNLO results for all of the form factors. Other effects that enter at this order are relativistic corrections, radiation pions, and nucleon form factors.

There remain a number of NLO calculations to be done in the two-nucleon system, and we are optimistic about their success. Extending this procedure to the three-body system and beyond remains a fascinating challenge [20].

ACKNOWLEDGMENTS

We thank G. Rupak and N. Shoresh for showing us a simple way to compute some of the Feynman graphs we encountered. This work was supported in part by the U.S. Department of Energy under Grants No. DOE-ER-40561, DE-FG03-97ER4014, and DE-FG03-92-ER40701.

APPENDIX A: THE GRAPHICAL EXPANSION OF THE MATRIX ELEMENT OF J^μ_{em}

1. Irreducible Green's functions

In this appendix we derive Eq. (3.5) which is central to our calculation of the deuteron electromagnetic form factors. We begin with the interpolating field defined in the text

$$\mathcal{D}_i \equiv N^T P_i N, \tag{A1}$$

where P_i is the projection defined in eq. (2.14). The full propagator G is defined as the time ordered product of two of these $\mathcal{D}$ fields:

$$G(\overline{E})\,\delta_{ij} = \int d^4x e^{-i(Et-\mathbf{p}\cdot\mathbf{x})} \langle 0|\mathrm{T}[\mathcal{D}_i^\dagger(x)\mathcal{D}_j(0)]|0\rangle = \delta_{ij}\frac{i\mathcal{Z}(\overline{E})}{\overline{E}+B+i\varepsilon}, \tag{A2}$$

where B is the deuteron binding energy. By Lorentz invariance, the propagator only depends on the energy in the center-of-mass frame, namely

$$\overline{E} \equiv E - \frac{\mathbf{p}^2}{4M} + \cdots, \quad E \equiv (p^0 - 2M), \tag{A3}$$

where the ellipsis refers to relativistic corrections to the dispersion relation. The numerator $\mathcal{Z}$ in Eq. (A2) is assumed to be smooth near the deuteron pole, and when evaluated at the pole gives the wave-function renormalization Z,

$$\mathcal{Z}(-B) \equiv Z = -i\left[\frac{dG^{-1}(\overline{E})}{dE}\right]^{-1}_{\overline{E}=-B}. \tag{A4}$$

It is convenient to define ''irreducible'' Green's functions as the sum of graphs which do not fall apart when the graph is cut between incoming and outgoing nucleons at the four-fermion vertices proportional to C_0. The irreducible two-point function is denoted by Σ, and has the expansion shown in Fig. 1. One can see graphically (Fig. 6) that the relation between G and Σ is

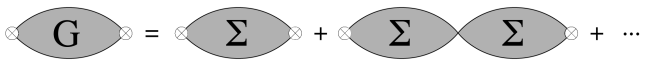

FIG. 6. The expansion of of the full two-point function G in terms of the irreducible two-point function Σ.

$$G = \frac{\Sigma}{1 + iC_0\Sigma}. \tag{A5}$$

It follows that

$$\Sigma|_{\overline{E}=-B} = \frac{i}{C_0}, \quad \frac{1}{\Sigma^2}\frac{d\Sigma}{dE}\bigg|_{\overline{E}=-B} = \frac{i}{Z}. \tag{A6}$$

In general, unphysical quantities such as Z, C_0, the deuteron wave function, etc. will depend on the renormalization scale μ, while S-matrix elements will be μ independent.

In order to compute the matrix element of the electromagnetic current between two deuteron states, we first define the three-point function

$$G^\mu_{ij}(\overline{E},\overline{E}',\mathbf{q}) = \int d^4x\, d^4y\, e^{-i(Ex^0-\mathbf{p}\cdot\mathbf{x})} e^{i(E'y^0-\mathbf{p}'\cdot\mathbf{y})} \times \langle 0|\mathrm{T}[\mathcal{D}_i^\dagger(x) J^\mu_{em}(0)\mathcal{D}_j(y)]|0\rangle, \tag{A7}$$

where $q^\mu = (E'-E, \mathbf{p}'-\mathbf{p})$ is the photon momentum. G^μ is related to the desired form factor via the LSZ formula

$$\langle \mathbf{p}', j|J^\mu_{em}|\mathbf{p}, i\rangle = Z[G^{-1}(\overline{E})G^{-1}(\overline{E}')G^\mu_{ij}(\overline{E},\overline{E}',\mathbf{q})]_{\overline{E},\overline{E}'\to -B}, \tag{A8}$$

where $G(\overline{E})$ is defined in Eq. (A2). It is convenient to reexpress this formula in terms Σ and the irreducible three-point function, which we call Γ^μ. It is easy to see graphically (Fig. 7) that the relation between G^μ and Γ^μ is

$$G^\mu_{ij}(\overline{E},\overline{E}',\mathbf{q}) = \frac{\Gamma^\mu_{ij}(\overline{E},\overline{E}',\mathbf{q})}{[1+iC_0\Sigma(\overline{E})][1+iC_0\Sigma(\overline{E}')]} = \frac{\Gamma^\mu_{ij}(\overline{E},\overline{E}',\mathbf{q})G(\overline{E})G(\overline{E}')}{\Sigma(\overline{E})\Sigma(\overline{E}')}. \tag{A9}$$

Making use of this relation and Eqs. (A5),(A6),(A8) allows us to reexpress the matrix element of the current in terms of Γ^μ and Σ:

$$\langle \mathbf{p}', j|J^\mu_{em}|\mathbf{p}, i\rangle = Z\left[\frac{\Gamma^\mu_{ij}(\overline{E},\overline{E}',\mathbf{q})}{\Sigma(\overline{E})\Sigma(\overline{E}')}\right]_{\overline{E},\overline{E}'\to -B} = i\left[\frac{\Gamma^\mu_{ij}(\overline{E},\overline{E}',\mathbf{q})}{d\Sigma(\overline{E})/dE}\right]_{\overline{E},\overline{E}'\to -B}. \tag{A10}$$

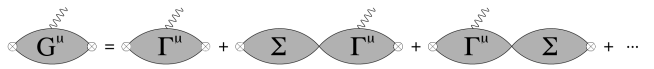

FIG. 7. The expansion of full three-point function G^μ in terms of the irreducible two- and three-point functions Σ, Γ^μ.

It is this relation that has a simple perturbative description in terms of Feynman graphs.

2. Computing Σ

We can now compute Σ in our perturbative expansion, writing Σ as

$$\Sigma(\bar{E}) = \sum_{n=1}^{\infty} \Sigma_{(n)}(\bar{E}), \tag{A11}$$

where $\Sigma_{(n)}(\bar{E}) \sim O(Q^n)$. The leading contribution to Σ is shown in the first row of Fig. 1, and is $O(Q)$ according to the rules of the previous section. These graphs are readily evaluated using the formula Eq. (2.16), with the result

$$\Sigma_{(1)}(\bar{E}) = -i\frac{M}{4\pi}(\mu - \sqrt{-M\bar{E} - i\varepsilon}). \tag{A12}$$

The subleading contribution is $O(Q^2)$ and one must compute the three graphs shown in the second row of Fig. 1. The result is [1]

$$\begin{aligned}\Sigma_{(2)}(\bar{E}) = -i\frac{g_A^2 M^2 m_\pi^2}{32\pi^2 f^2}\Bigg[& i\tan^{-1}\left(\frac{2\sqrt{M\bar{E}}}{m_\pi}\right) \\ & -\frac{1}{2}\ln\left(\frac{m_\pi^2 + 4M\bar{E}}{\mu^2}\right) + 1\Bigg] \\ & -i\left(\frac{g_A^2}{2f^2} + C_2 M\bar{E} + D_2 m_\pi^2\right)[\Sigma_{(1)}(\bar{E})]^2.\end{aligned} \tag{A13}$$

To the order we are working we truncate the expansion in Eq. (3.6) to the nonrelativistic result

$$\bar{E} \simeq E - \frac{\mathbf{p}^2}{4M}; \tag{A14}$$

the first relativistic correction enters at NNLO, or $O(Q^3)$. Other NNLO contributions are shown in the third row of Fig. 1, and include the exchange of two potential pions, or one radiative pion (see [1] for discussion) as well as several other graphs.

From Eq. (3.5) we see that what is needed is $d\Sigma/d\bar{E}$ evaluated at $\bar{E} = -B$. From Eqs. (A12) and (A13) we find

$$\left.\frac{d\Sigma_{(1)}}{d\bar{E}}\right|_{\bar{E}=-B} = -i\frac{M^2}{8\pi\gamma},$$

$$\begin{aligned}\left.\frac{d\Sigma_{(2)}}{d\bar{E}}\right|_{\bar{E}=-B} = -i\frac{M^3}{16\pi^2\gamma}\Bigg[& \frac{g_A^2}{2f^2}\left(\gamma - \mu + \frac{m_\pi^2}{m_\pi + 2\gamma}\right) \\ & + D_2 m_\pi^2(\gamma - \mu) - C_2\gamma(\mu - \gamma)(\mu - 2\gamma)\Bigg],\end{aligned} \tag{A15}$$

where we have defined

$$\gamma \equiv \sqrt{MB}. \tag{A16}$$

3. Computing Γ^0

The leading contribution to the matrix element of the J^0_{em} current between deuteron states arises from the three-point function $\Gamma^0_{(-1)}$, the first graph in Fig. 2,

$$\Gamma^0_{(-1)} = -e\,\delta_{ij}\frac{M^2}{2\pi q}\tan^{-1}\left(\frac{q}{4\gamma}\right), \tag{A17}$$

where $q = |\mathbf{q}|$ is the magnitude of the photon three-momentum, and γ was defined above in Eq. (A16).

At subleading order we need to sum the diagrams in the second row of Fig. 2. In each case, there is a minimally coupled A_0 photon coupled to the proton propagator, with either an insertion of the C_2 or D_2 contact interactions, or a single pion exchange.[4] We find

$$\begin{aligned}\Gamma^0_{(0)} = e\,\delta_{ij}\frac{M^3}{16\pi^2}\Bigg\{ & D_2(\mu)\frac{4m_\pi^2(\mu-\gamma)}{q}\tan^{-1}\left(\frac{q}{4\gamma}\right) + C_2(\mu)(\mu-\gamma)\left[\mu - \gamma - \frac{4\gamma^2}{q}\tan^{-1}\left(\frac{q}{4\gamma}\right)\right] \\ & + \left(\frac{g_A}{f}\right)^2\left[\frac{2(\mu-\gamma)}{q}\tan^{-1}\left(\frac{q}{4\gamma}\right) - \int_0^1 dx\,\frac{m_\pi^2}{xq\Delta(x)}\tan^{-1}\left(\frac{xq}{2[\Delta(x)+\gamma+m_\pi]}\right)\right]\Bigg\} \\ & + e(\mathbf{q}_i\mathbf{q}_j - q^2\delta_{ij})\frac{9g_A^2M^3}{16\pi^2 f^2 q^3}\int_0^1 dx\int_0^\infty dr\,\frac{e^{-[\Delta(x)+\gamma+m_\pi]r}}{xr^3\Delta(x)}(3 + 3m_\pi r + m_\pi^2 r^2) \\ & \times\left[\frac{2}{xqr}\cos\left(\frac{xqr}{2}\right) + \left(\frac{1}{3} - \frac{4}{x^2q^2r^2}\right)\sin\left(\frac{xqr}{2}\right)\right],\end{aligned} \tag{A18}$$

[4] One might worry that in fact there are four-nucleon contact interactions involving the combination a covariant time derivative D_0, and hence a direct photon coupling to the $N^\dagger N^\dagger NN$ vertex. In fact, such an operator may be eliminated by using the equations of motion. We demonstrate this by explicit calculation in Appendix B.

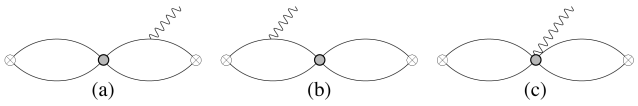

FIG. 8. Feynman diagrams contributing to the matrix element (denoted by the gray circle) of the operator $\mathcal{O}$ in Eq. (B1).

where $\Delta(x)$ is defined in Eq. (3.13).

As discussed in the text, the calculation of the parts of Γ^i which are antisymmetric in the deuteron polarizations is completely analogous to the complete calculation of Γ^0 presented here.

APPENDIX B: NO OFF-SHELL AMBIGUITY — AN EXPLICIT COMPUTATION

When working with potential models for NN interactions one often faces ambiguities about how to continue matrix elements off-shell. In an effective field theory approach, there is no such ambiguity. All uncertainties arising in a consistent calculation are due to higher-order operators neglected at the order one is working [21]. To illustrate this, we consider the effect of the operator

$$\mathcal{O}=(N^T P_i N)^\dagger\left\{ iD_0(N^T P_i N)+\left[\left(\frac{\mathbf{D}^2}{2M}N^T\right)P_i N + N^T P_i\left(\frac{\mathbf{D}^2}{2M}N\right)\right]\right\}, \tag{B1}$$

where D_μ is the gauge covariant derivative[5]

$$D_\mu=\partial_\mu+ieQ_{em}A_\mu, \tag{B2}$$

Q_{em} being the electric charge matrix. The operator $\mathcal{O}$ is not Galilean invariant but nonetheless we can, in principle, consider how it enters the NLO calculation of the deuteron form factors via the graphs in Fig. 8. However, to the order we are working, it vanishes by the equations of motion,

$$\left(iD_0+\frac{\mathbf{D}^2}{2M}\right)N(\mathbf{x},t)=0. \tag{B3}$$

One might naively think that the equations of motion imply that the operator $\mathcal{O}$ will not enter a calculation of NN phase shifts (as the nucleons are on-shell in that process), yet that $\mathcal{O}$ will affect deuteron matrix elements, since the nucleons are not on-shell in a bound state. This would mean that a new constant enters the deuteron calculation which cannot be determined via NN scattering.

However, this is reasoning is incorrect, and we now show by explicit calculation that operator $\mathcal{O}$ does indeed vanish when considering deuteron matrix elements. This result is consistent with general theorems of field theory that state that off-shell matrix elements are arbitrary (they can be changed by making a field redefinition) and that the S-matrix elements never depend on them (even when the matrix element is between bound states).

As an example, consider the contribution to the deuteron three-point function Γ^0 of the operator $\mathcal{O}$ in the graphs of Fig. 8, corresponding to the matrix element

$$\Gamma^0=\langle 0|T[\mathcal{D}_i^\dagger(E,\mathbf{0})\mathcal{D}_j(E',\mathbf{q})A^0(q^0,\mathbf{q})]|0\rangle, \tag{B4}$$

where $E'=E+q^0$. The first graph, Fig. 8(a), includes the photon-independent part of $\mathcal{O}$ and a minimally coupled A^0 photon on a nucleon leg. It is proportional to

$$\begin{aligned}(\mathrm{a})\propto -i\int\frac{d^{D-1}\mathbf{k}}{(2\pi)^{D-1}}\frac{d^{D-1}\mathbf{l}}{(2\pi)^{D-1}} &\times\frac{E-\mathbf{k}^2/M}{(E-\mathbf{k}^2/M)(E-\mathbf{l}^2/M)(E'-[\mathbf{l}^2+(\mathbf{l}+\mathbf{q})^2]/2M)}\\ &=0,\end{aligned} \tag{B5}$$

where $D\to 4$ at the end of the calculation. To evaluate this integral, we used the fact that the first term in the numerator cancels the first propagator, and that in dimensional regularization

$$\int\frac{d^{D-1}\mathbf{k}}{(2\pi)^{D-1}}=0. \tag{B6}$$

The second graph in Fig. 8 is similar, and proportional to

$$\begin{aligned}(\mathrm{b})\propto -i\int\frac{d^{D-1}\mathbf{k}}{(2\pi)^{D-1}}\frac{d^{D-1}\mathbf{l}}{(2\pi)^{D-1}}&\frac{E'-[\mathbf{k}^2+(k+q)^2]/2M}{(E-\mathbf{k}^2/M)(E'-[\mathbf{k}^2+(\mathbf{k}+\mathbf{q})^2]/2M)(E'-[\mathbf{l}^2+(\mathbf{l}+q)^2]/2M)}\\ =-i\int\frac{d^{D-1}\mathbf{k}}{(2\pi)^{D-1}}\frac{d^{D-1}\mathbf{l}}{(2\pi)^{D-1}}&\frac{1}{(E-\mathbf{k}^2/M)(E'-[\mathbf{l}^2+(\mathbf{l}+q)^2]/2M)}.\end{aligned} \tag{B7}$$

[5]To be chirally invariant, the covariant derivative should include pion fields, but as the pion couplings do not enter to the order we are working, we have set them to zero.

Finally, the third graph, Fig. 8(c), arises from the A^0 photon coupling in $\mathcal{O}$, and gives

$$(\mathrm{c}) \propto + i \int \frac{d^{D-1}\mathbf{k}}{(2\pi)^{D-1}} \frac{d^{D-1}\mathbf{l}}{(2\pi)^{D-1}} \times \frac{1}{(E-\mathbf{k}^2/M)(E'-[\mathbf{l}^2+(\mathbf{l}+q)^2]/2M)}. \quad \text{(B8)}$$

It follows that the sum of the three graphs in Fig. 8 vanishes, and there is no off-shell ambiguity arising from this new operator $\mathcal{O}$. Similar remarks hold for other operators with a single time derivative. Therefore, we can choose to only include the two spatial derivative operators in the Lagrangian (our interaction proportional to C_2) and to eliminate the analogous operators with a time derivative by the equations of motion — *even though we are considering nucleons bound in a deuteron.* This result is not peculiar to the particular regularization scheme we used.

[1] D.B. Kaplan, M.J. Savage, and M.B. Wise, Phys. Lett. B **424**, 390 (1998); Nucl. Phys. **B534**, 329 (1998).

[2] A.V. Manohar, Lectures given at 35th Internationale Universitatswochen fuer Kern- und Teilchenphysik, Perturbative and Nonperturbative Aspects of Quantum Field Theory, Schladming, Austria, 1996, hep-ph/9606222.

[3] C. Ordóñez, L. Ray, and U. van Kolck, Phys. Rev. C **53**, 2086 (1996).

[4] T.-S. Park, K. Kubodera, D.-P. Min, and M. Rho, Phys. Rev. C **58**, 637 (1998).

[5] H.A. Bethe, Phys. Rev. **76**, 38 (1949).

[6] H.A. Bethe and C. Longmire, Phys. Rev. **77**, 647 (1950).

[7] T. Ericson, Nucl. Phys. **A416**, 281c (1984).

[8] T. Ericson and M. Rosa-Clot, Annu. Rev. Nucl. Part. Sci. **35**, 271 (1985).

[9] E. Jenkins, M. Luke, A.V. Manohar, and M.J. Savage, Phys. Lett. B **302**, 482 (1993); **388**, 866(E) (1996), and references therein.

[10] S. Weinberg, Phys. Lett. B **251**, 288 (1990); Nucl. Phys. **B363**, 3 (1991); Phys. Lett. B **295**, 114 (1992).

[11] See, for example, M. J. Zuilhof and J. A. Tjon, Phys. Rev. C **22**, 2369 (1980).

[12] A.J. Buchmann, H. Henning, and P.U. Sauer, Few-Body Syst. **21**, 149 (1996).

[13] T. Ericson and W. Weise, *Pions and Nuclei* (Oxford University Press, Oxford, 1988).

[14] D.Y. Wong, Phys. Rev. Lett. **2**, 406 (1959).

[15] B.S. Pudliner, V.R. Pandharipande, J. Carlson, S.C. Pieper, and R.B. Wiringa, nucl-th/9705009.

[16] G. G. Simon, CH. Schmitt, and V. H. Walther, Nucl. Phys. **A364**, 285 (1981).

[17] B. Grosstete, D. Drickey, and P. Lehmann, Phys. Rev. **141**, 1425 (1966).

[18] D. Benaksas, D. Drickey, and D. Frerejacque, Phys. Rev. **148**, 1327 (1966).

[19] D. Ganichot, B. Grosstete, and D. B. Isabelle, Nucl. Phys. **A178**, 545 (1972).

[20] P. F. Bedaque and U. Van Kolck, Phys. Lett. B **428**, 221 (1998); P. F. Bedaque, H.-W. Hammer, and U. Van Kolck, Phys. Rev. C **58**, R641 (1998).

[21] H. D. Politzer, Nucl. Phys. **B172**, 349 (1980); C. Arzt, Phys. Lett. B **342**, 189 (1995).